Electronic Supplementary Information

Rational design of Pt-Ni-Co ternary alloy nanoframe crystals as highly efficient catalysts toward alkaline hydrogen evolution reaction

Aram Oh,[a,b,‡] Young Jin Sa,[c,‡] Hyeyoun Hwang,[a,b,‡] Hionsuck Baik,[d] Jun Kim,[a,b] Byeongyoon Kim,[a,b] Sang Hoon Joo*[c] and Kwangyeol Lee*[a,b]

[a] Center for Molecular Spectroscopy and Dynamics, Institute for Basic Science (IBS), Seoul 02841, Korea

[b] Department of Chemistry and Research Institute of Natural Sciences, Korea University, Seoul 02841 , Korea, E-mail: kylee1@korea.ac.kr

[c] Department of Chemistry, Ulsan National Institute of Science and Technology (UNIST), Ulsan 44919, Korea, E-mail: shjoo@unist.ac.kr

[d] Korea Basic Science Institute (KBSI), Seoul 02841, Korea

‡These authors contributed equally to this paper.

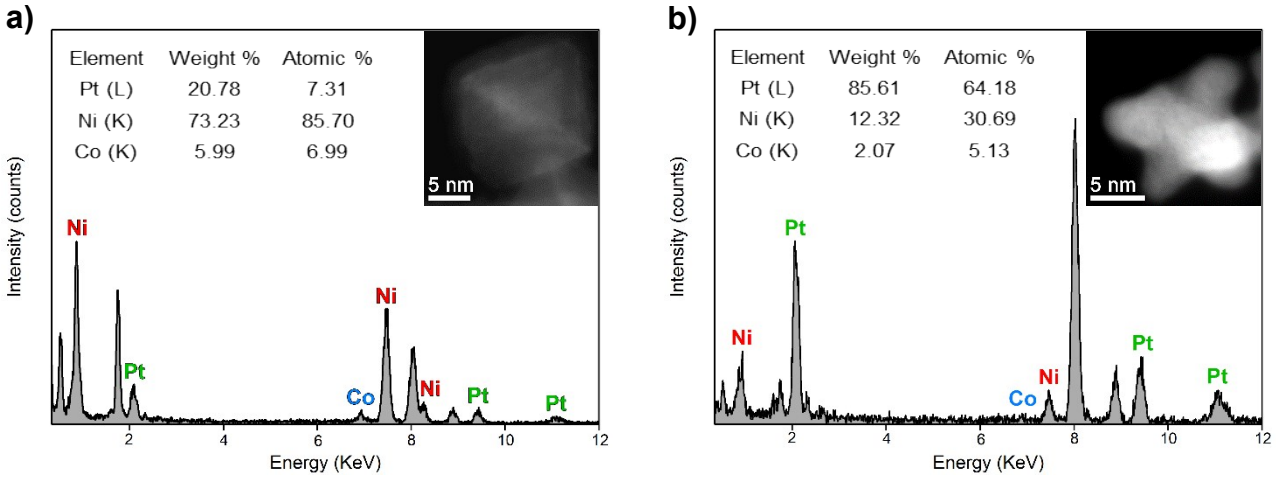

Fig. S1. Quantitative EDS analysis of (a) PNC and (b) PNCH. While (a) PNC, the original synthetic product, exhibits the Ni as the major component in the phase-segregated nanostructure, Pt becomes the major component for (b) PNCH after chemical etching process. The non-marginal presence of Ni and Co component in the final etched product of PNCH indicates the formation of Pt-rich PtNiCo alloy, likely Pt/Ni/Co solid solution, structures.

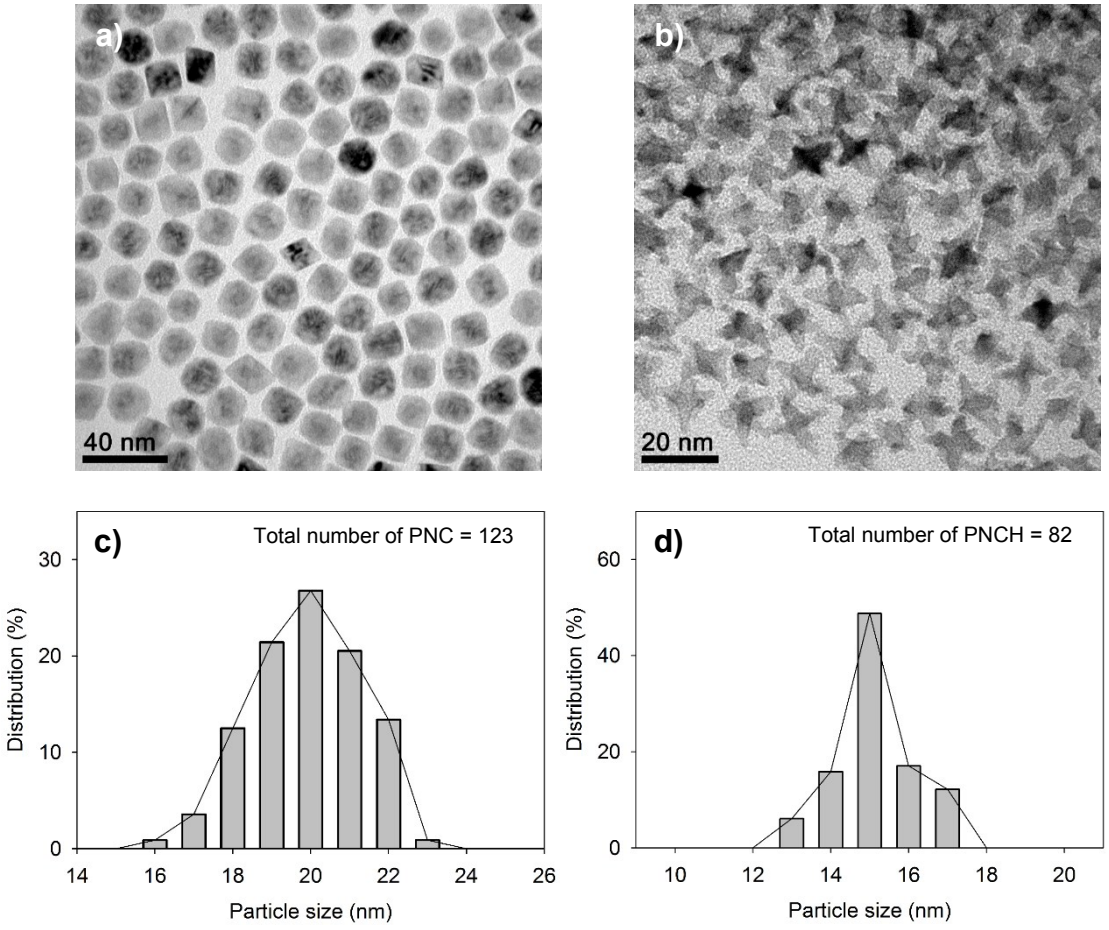

Fig. S2. TEM images of nanostructures of (a) PNC and (b) PNCH and (c and d) their corresponding histograms for particle size distributions. The histograms for PNC and PNCH show narrow size distribution mainly from 18 to 22 nm and 13 to 17 nm, respectively.

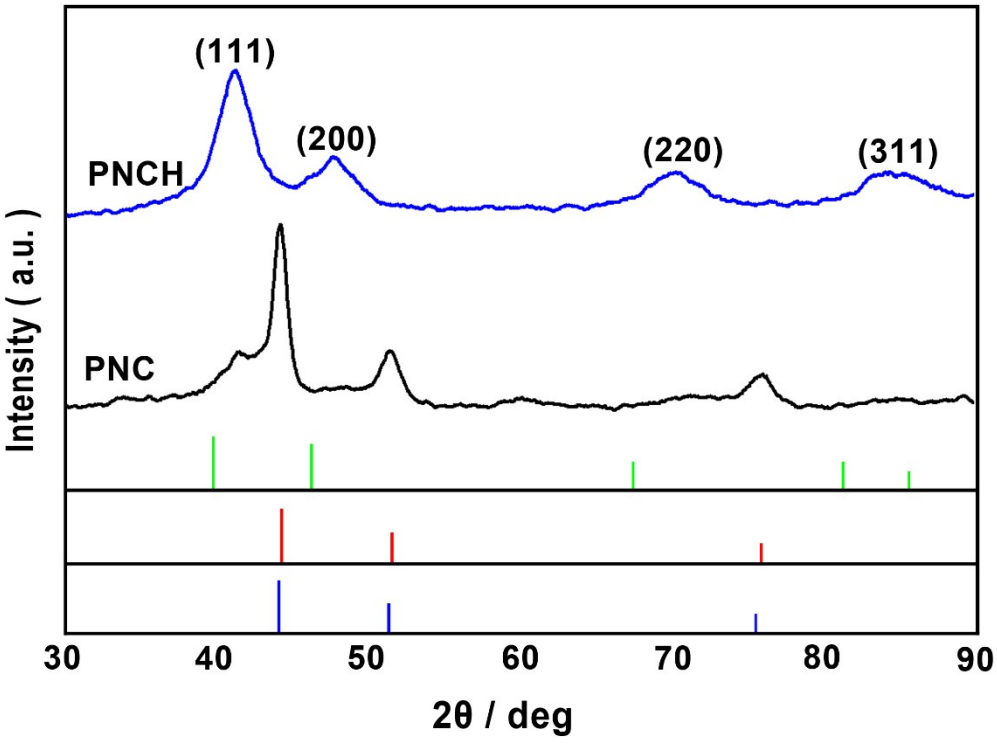

Fig. S3. X-ray diffraction patterns of PNC and PNCH. Color sticks indicate the X-ray diffraction lines for references: green, Pt (ICSD no. 64923); red, Ni (ICSD no. 53807); blue, Co (ICSD no. 53805).

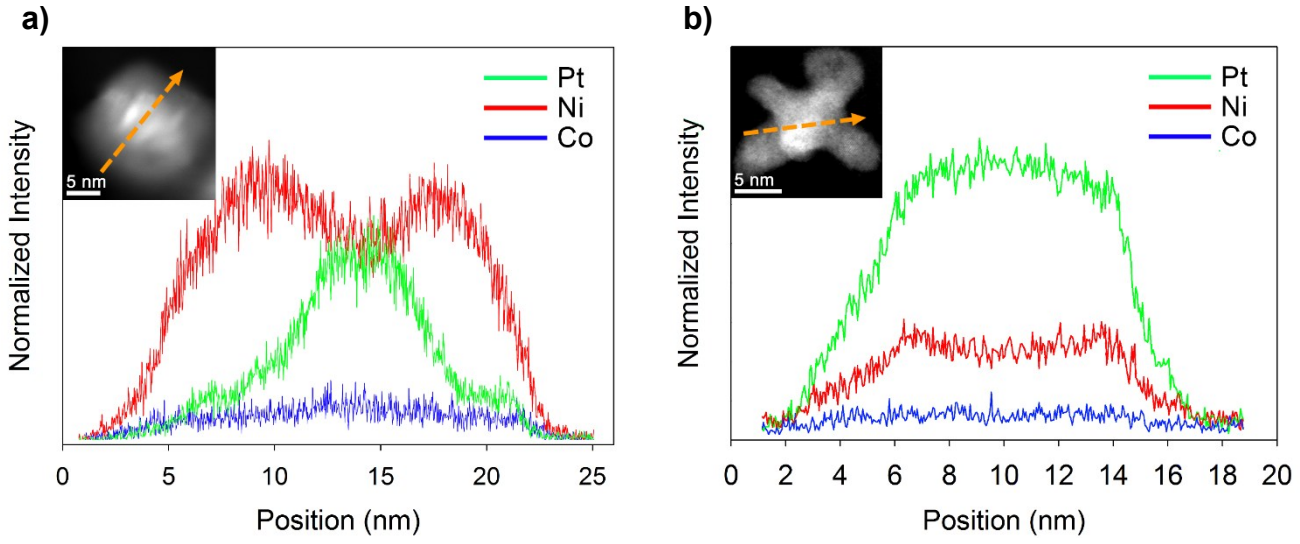

Fig. S4. HAADF STEM images and EDS line-scanning profile analysis of as-synthesized (a) PNC and (b) PNCH nanostructures. The orange arrows in the STEM images indicate line scan directions for the corresponding nanostructures.

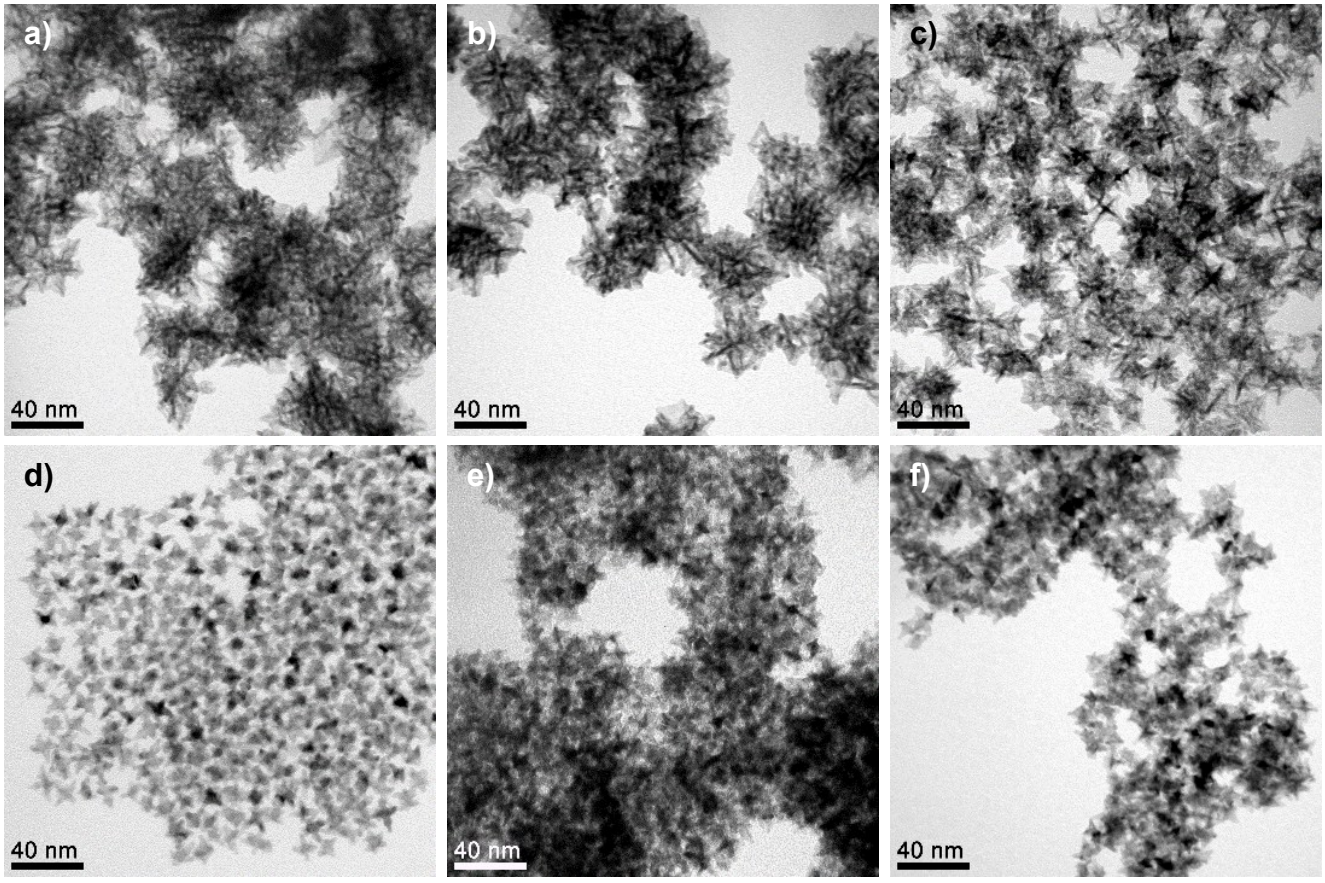

Fig. S5. TEM images for the structural evolution of Pt-rich nanoframes with different amount of the $CoCl_2$ precursors: (a) 0 equiv., (b) 1 equiv., (c) 3 equiv., (d) 5 equiv., (e) 7 equiv., and (f) 9 equiv.

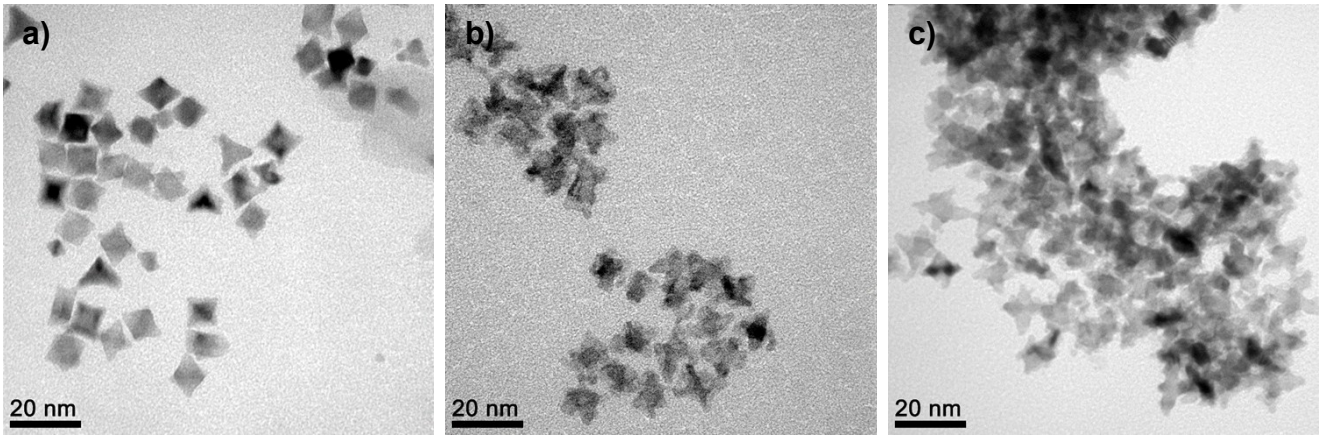

Fig. S6. TEM images of reaction intermediates after selective removal of Ni/Co-rich phase. The reaction time for each intermediate is (a) 2 min, (b) 5 min, and (c) 15 min.

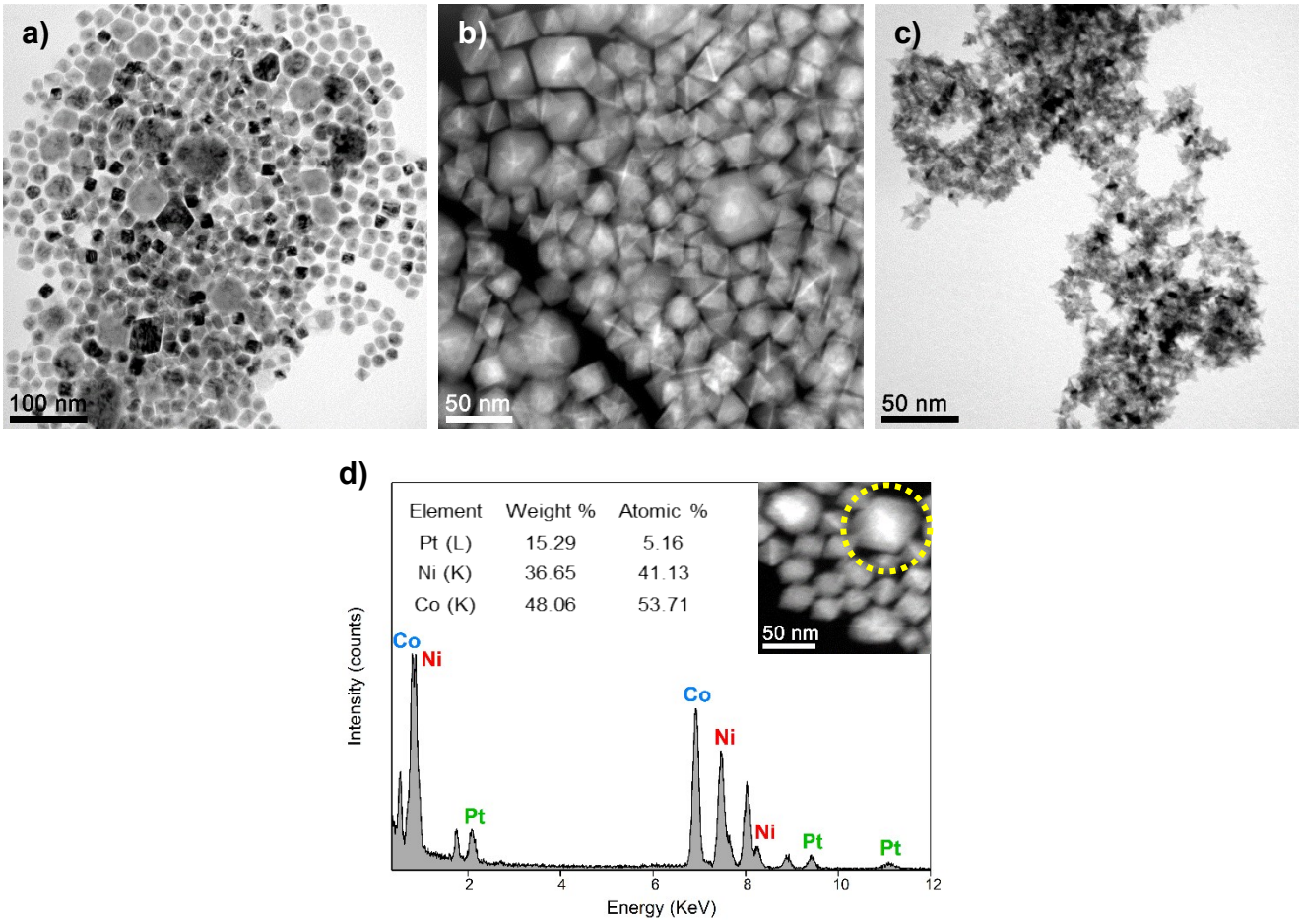

Fig. S7. Structural and component analysis of PNC and PNCH at 12 h. (a) TEM and (b) STEM images of PNC. (c) TEM image of PNCH. (d) EDS quantitative analysis of PNC with thick Co-shell in the yellow dotted circle of inset STEM image. Some PNCs have thicker Co-shell than the other PNCs. However, the sizes and shapes of the final PNCH are very similar after Ni/Co-phase removal.

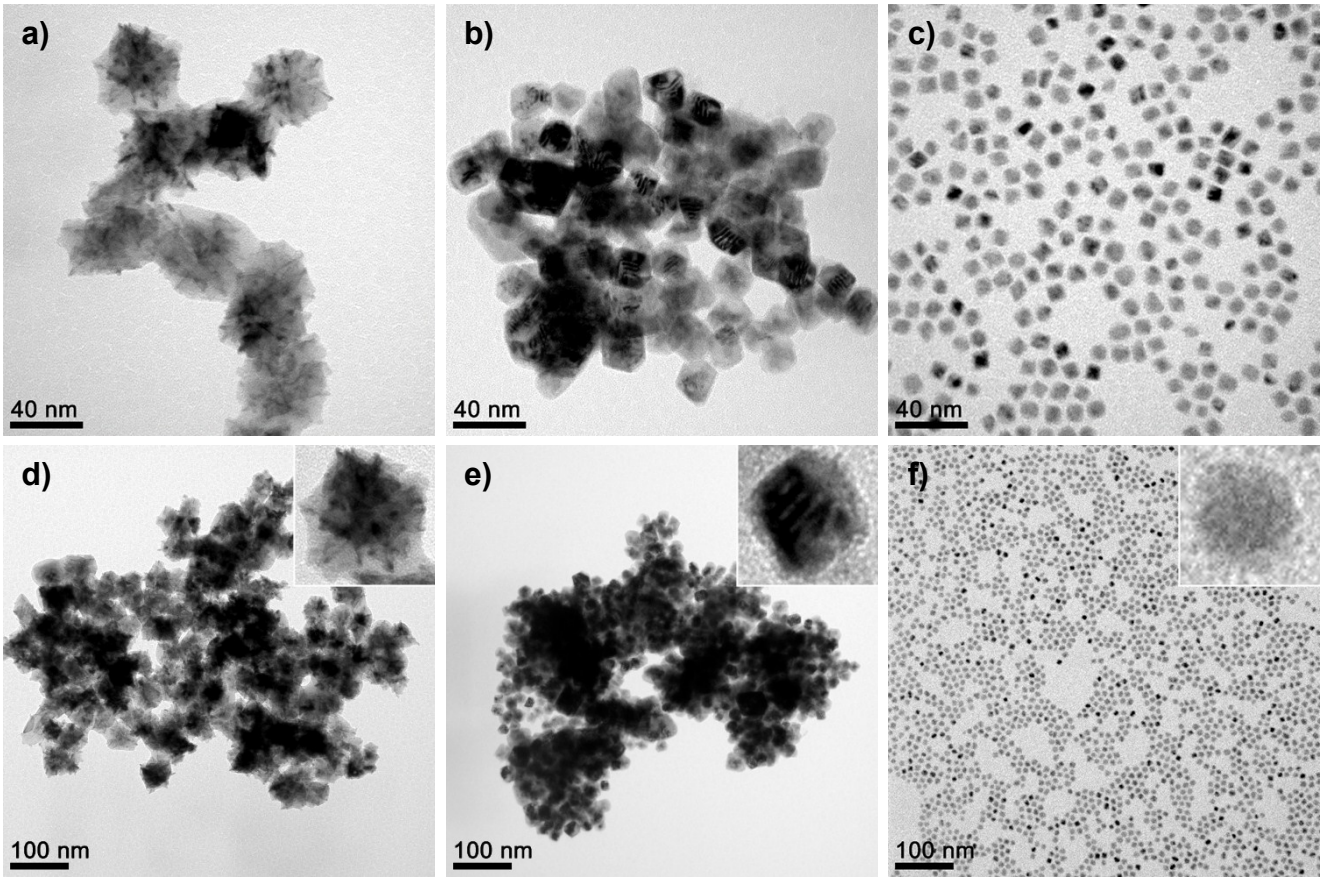

Fig. S8. TEM images of PNC obtained by different metal precursors. (a,d) with $Ni(acac)_2$ and $Co(acac)_3$, (b,e) with $NiCl_2$ and $Co(acac)_3$, (c,f) with $CoBr_2$ instead of $CoCl_2$. Insets of TEM images indicate the high magnification TEM images of the corresponding nanostructures.

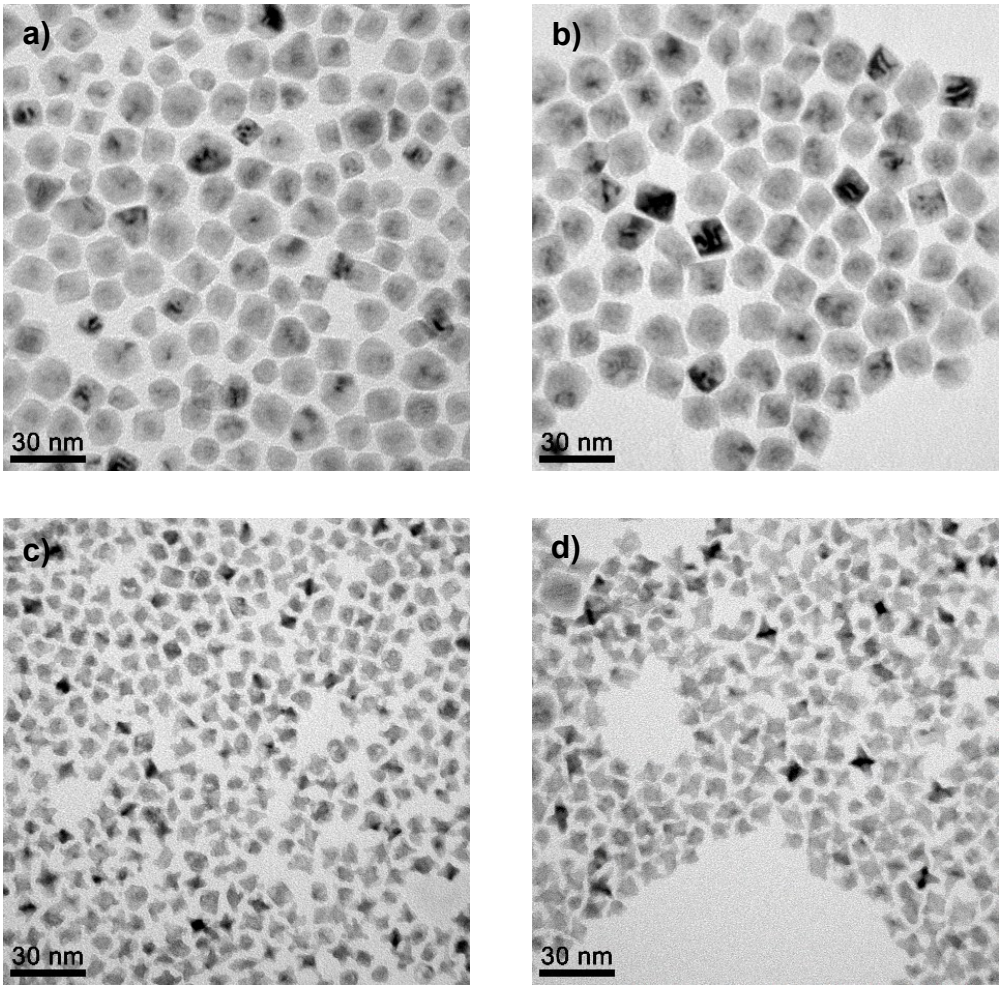

Fig. S9. TEM images of PNC (a,b) and PNCH (c,d) obtained without sodium oleate (a,c), without stearic acid (b,d). In the absence of sodium oleate or stearic acid, irregularly developed facet controlled nanocrystals of the octahedral nanostructure were observed. This indicates that sodium oleate and stearic acid assist indirectly well-defined facet-control of the nanocrystals.

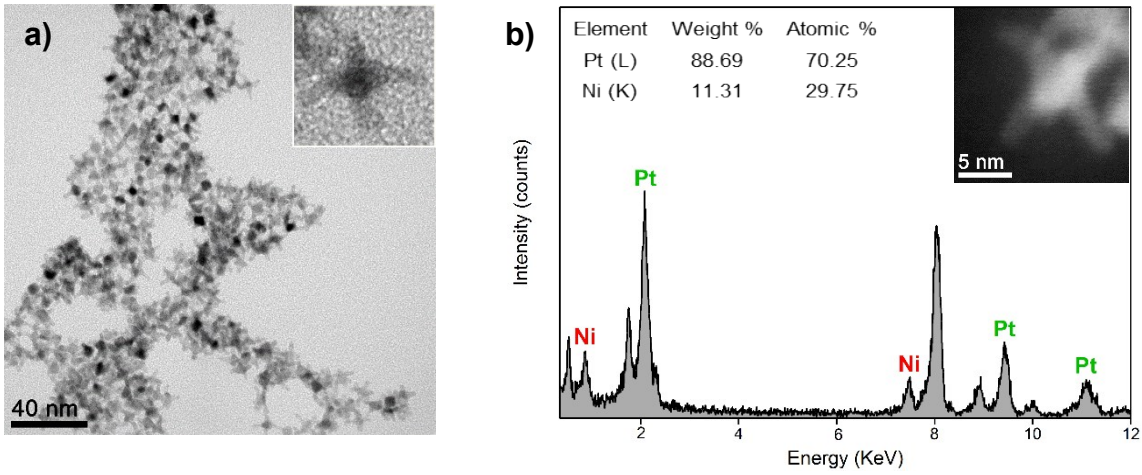

Fig. S10. Structural and component analysis of PNH. (a) TEM and (b) EDS quantitative analysis of PNH.

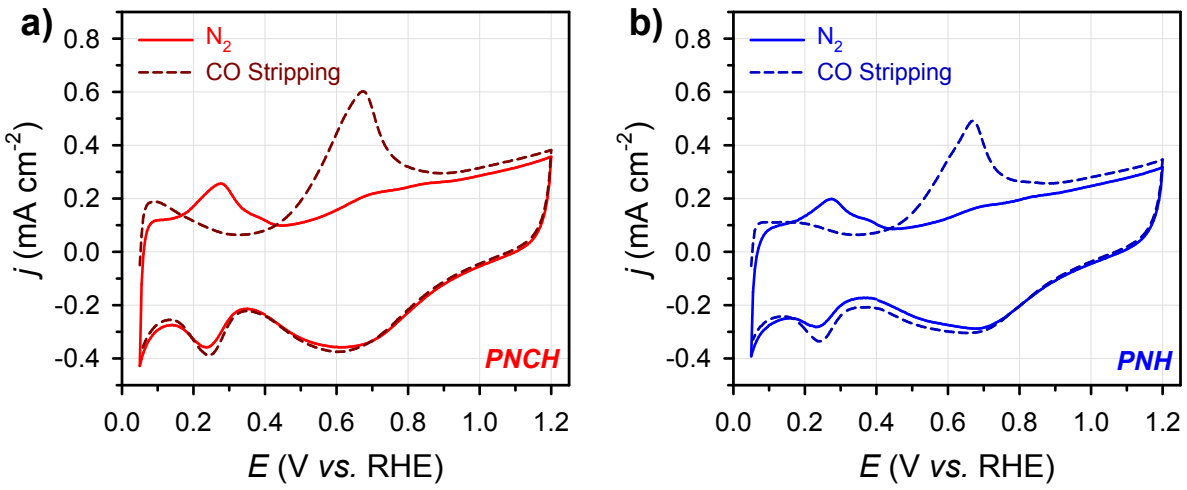

Fig. S11. Cyclic voltammograms (CVs) obtained before and after the adsorption of CO molecules on the Pt surface of (a) PNCH and (b) PNH in 0.1 M KOH at a scan rate of 50 mV s^{-1}.

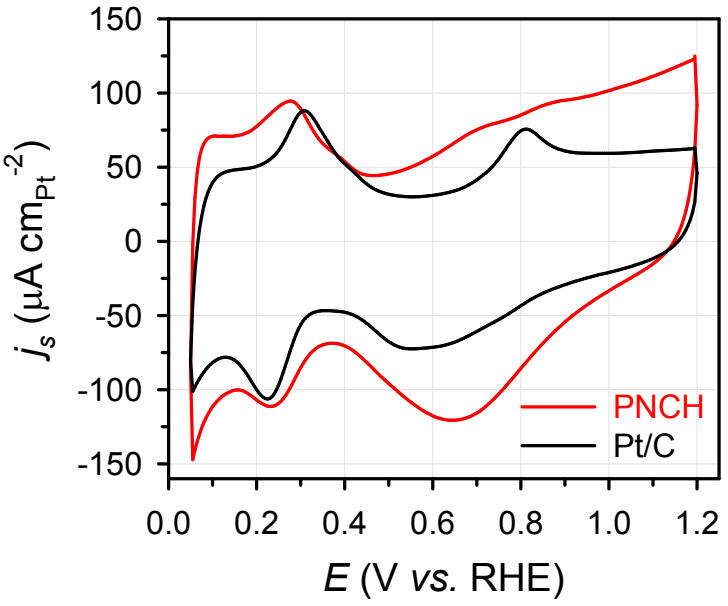

Fig. S12. Cyclic voltammograms (CVs) of PNCH and Pt/C catalysts normalized by Pt $ECSA_H$, obtained in N_2-saturated 0.1 M KOH

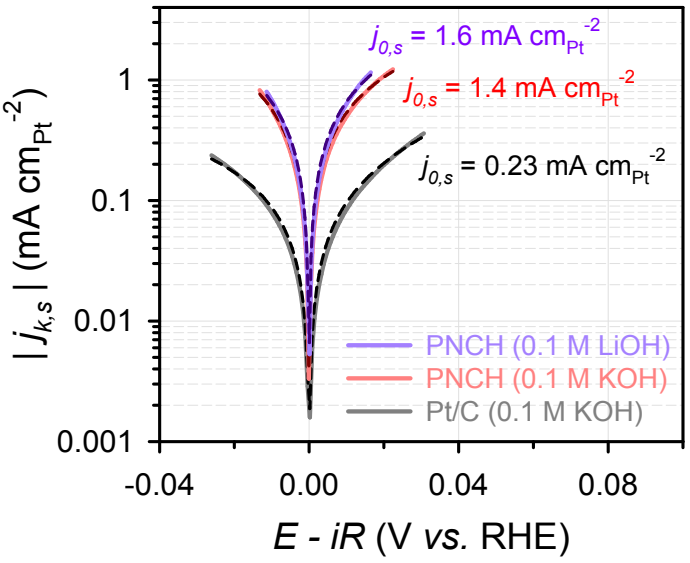

Fig. S13. Tafel plots for HER/HOR of PNCH obtained in 0.1 M KOH and 0.1 M LiOH, and Pt/C in 0.1 M KOH. Butler-Volmer fits are indicated by dashed curves. The specific current density was normalized by $ECSA_H$.

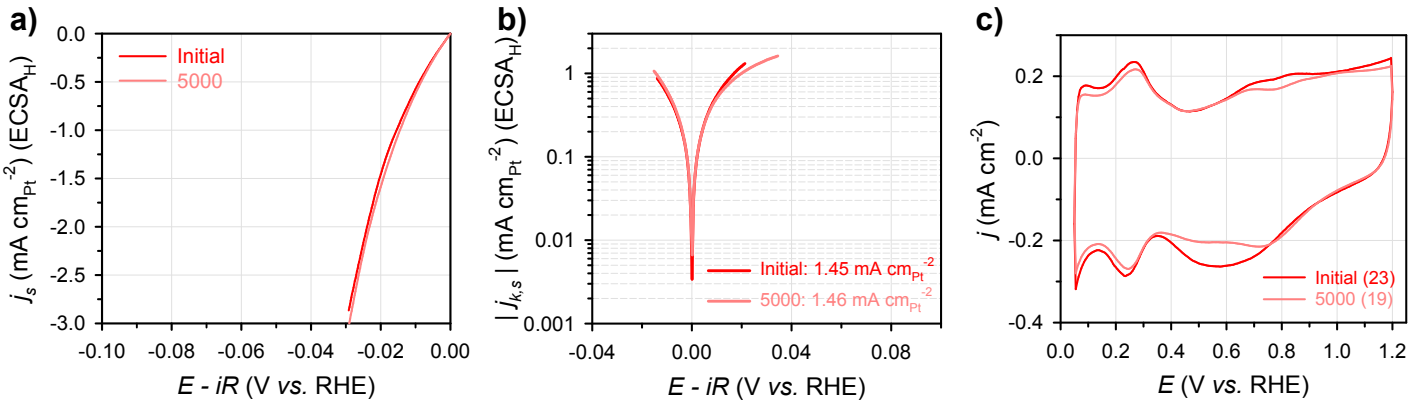

Fig. S14. HER activity of PNCH catalyst before and after 5,000 potential cycles from −0.3 V to 0.1 V at a scan rate of 50 mV s^{-1}. (a) HER polarization curves showing specific current densities normalized by Pt ECSA, (b) Tafel plots for HER/HOR, and exchange current densities from Butler-Volmer fitting. (c) CV curves before and after the cycling test. The numbers in the parentheses indicate $ECSA_H$.

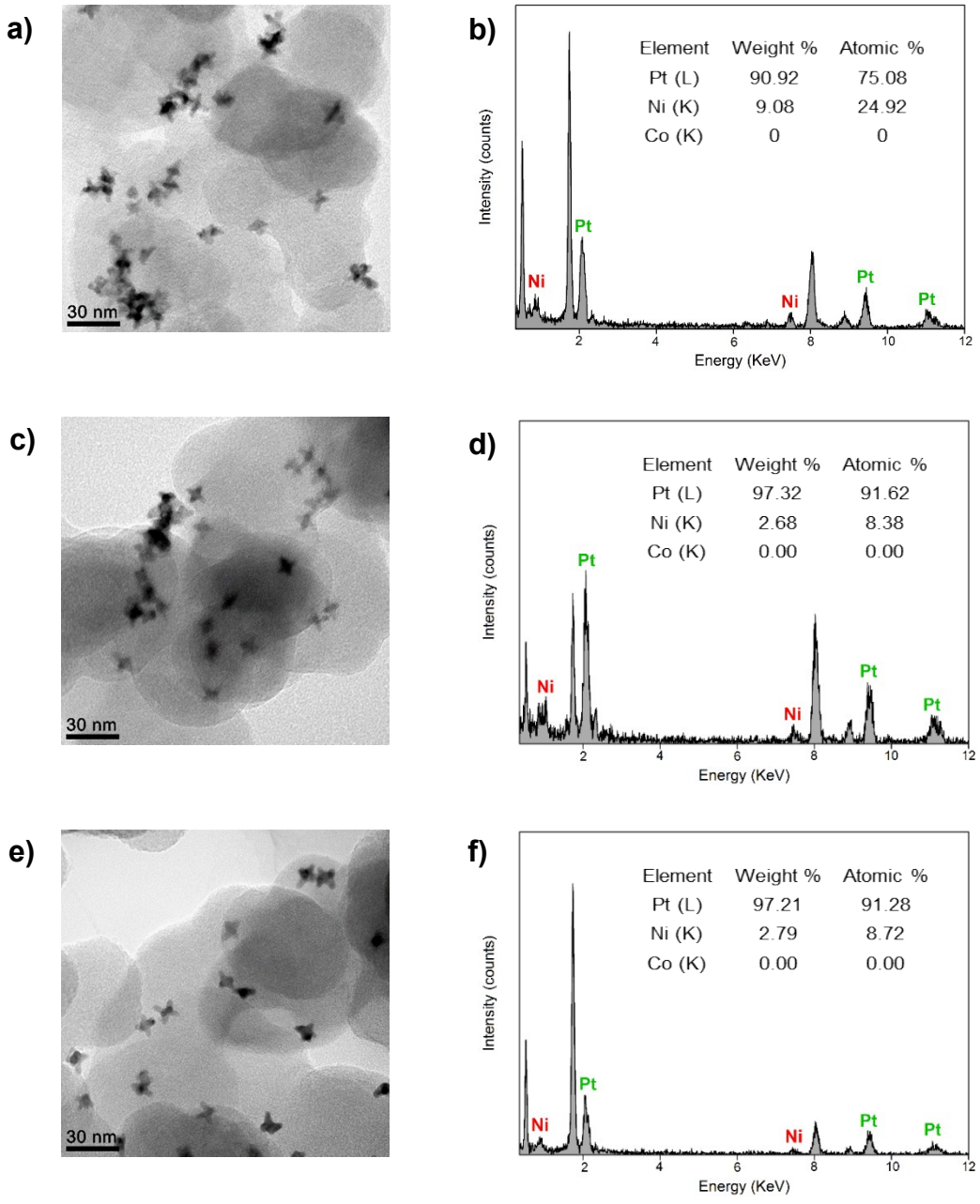

Fig. S15. TEM images and EDS quantitative analysis of PNCH after the electrochemical stability tests: (a,b) HER from -0.3 to 0.1 V, 50 mV s^{-1}, 5000 cycles, (c,d) ORR in N_2 from 0.6 to 1.0 V, 50 mV s^{-1}, 10000 cycles, (e,f) ORR in O_2 from 0.6 to 1.0 V, 50 mV s^{-1}, 10000 cycles.

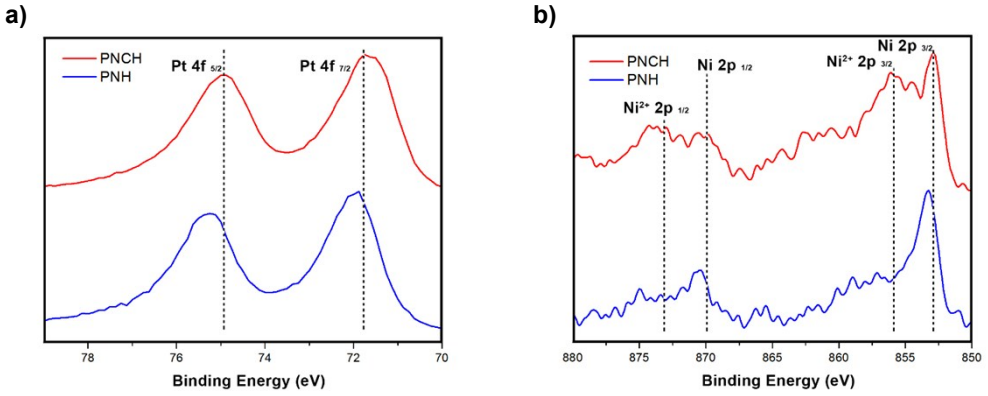

Fig. S16. XPS spectra of PNCH and PNH samples: (a) Pt 4f binding energy (b) Ni 2P binding energy.

Comment [O]: Fig. S16. (b)에서 Ni2+ ref. guideline 수정

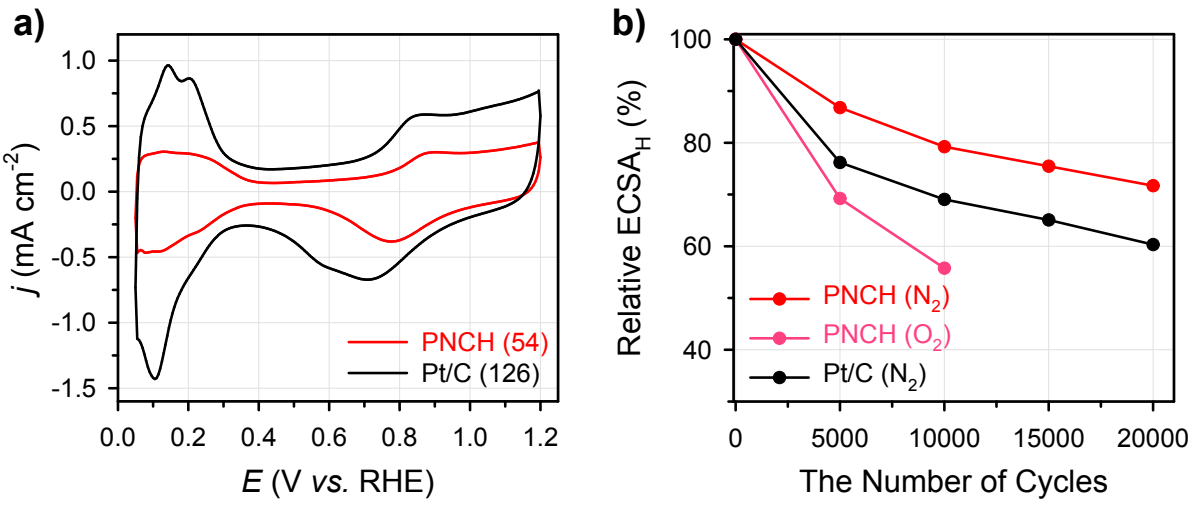

Fig. S17. (a) Cyclic voltammograms (CVs) of PNCH and Pt/C catalysts obtained in N_2-saturated 0.1 M $HClO_4$. The numbers in parentheses indicate the electrochemical surface area calculated from H desorption charge ($ECSA_H$). (b) Changes in relative electrochemical surface area (ECSA) of PNCH and Pt/C catalysts during 20,000 potential cycles from 0.6 V to 1.0 V in N_2-saturated 0.1 M $HClO_4$, and 10,000 potential cycles in O_2-saturated electrolyte (light red).

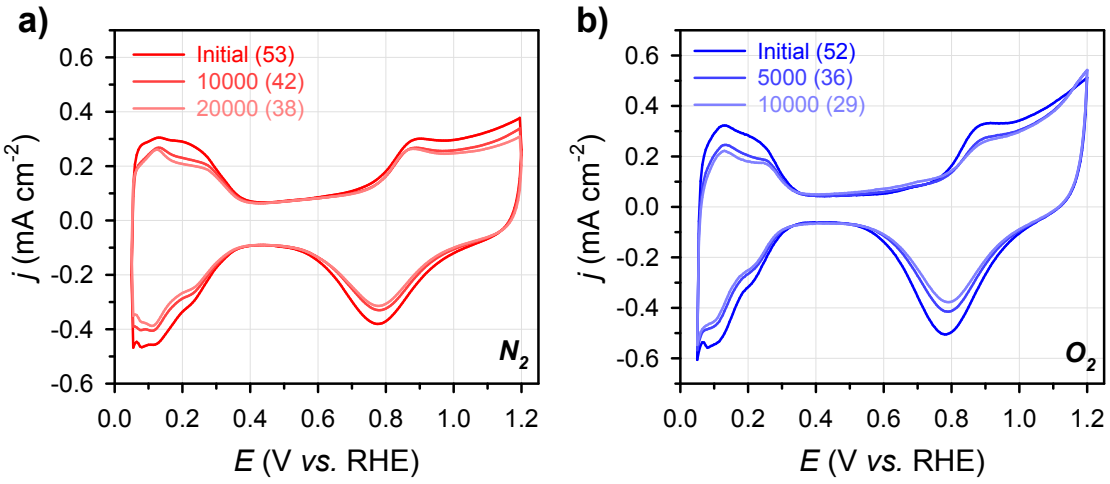

Fig. S18. Cyclic voltammograms (CVs) of PNCH after potential cycles in (a) N_2-saturated and (b) O_2-saturated 0.1 M $HClO_4$ at a scan rate of 50 mV s^{-1}. The numbers in the parentheses indicate $ECSA_H$.

Table S1. Comparison table showing experimental parameters and HER activities in terms of the overpotential at −5 mA cm^{-2}, specific current density at −0.02 V, and exchange current density from Butler-Volmer fitting.

Catalyst	Pt loading (μg cm^{-2})	Electrolyte	ECSA (m^2 g^{-1})	Potential @ −5 mA cm^{-2} (mV vs. RHE)	Specific Activity @ −20 mV (mA cm_{Pt}^{-2})	Exchange Current Density (mA cm_{Pt}^{-2})	Reference
PNCH	10	0.1 M KOH	24.7 (H-UPD)	−22	1.6	1.4	This work
			36 (CO)		1.0	0.9	This work
Pt/C	10	0.1 M KOH	85	−52	0.17	0.23	This work
PtCuNi/CNF@CF	N/A	1 M KOH	35.8	−150	N/A	N/A	S1
Ru@Pt (1ML)	17	1 M KOH	170	N/A	0.6	N/A	S2
$Ni(OH)_2$-Pt/C hybrid	1.13	0.1 M KOH	N/A	−157	N/A	N/A	S3
Pt NWs/SL-$Ni(OH)_2$	16	0.1 M KOH	22.8	−38	0.18	N/A	S4
PtNi frames/$Ni(OH)_2$	14	0.1 M KOH	N/A	−89	N/A	N/A	S5
Rh/Pt(poly)	N/A	0.1 M NaOH	N/A	−43	N/A	N/A	S6
Pt/Au/C	7	0.1 M KOH	4.1	N/A	N/A	0.7	S7
Pt/Cu nanowire	100	0.1 M KOH	35.9	−13	N/A	2.1	S8
Pt(111)-$Ni(OH)_2$	N/A	0.1 M KOH	N/A	−110	N/A	N/A	S9

Table S2. Summary of activity parameters, and exchange currents and transfer coefficient obtained from Butter-Volmer fitting.

Catalyst	*Pt loading* ($\mu g\ cm^{-2}$)	$ECSA_H$ ($m^2\ g^{-1}$)	j_0 [a] ($mA\ cm_{disk}^{-2}$)	$j_{0,s}$ [b] ($mA\ cm_{Pt}^{-2}$)	$j_{0,m}$ [c] ($A\ mg_{Pt}^{-1}$)	α [d]
PNCH	10	24.7 ± 0.5	3.42 ± 0.04	1.38 ± 0.03	0.34	0.42 ± 0.01
PNH	10	23.0 ± 1.1	2.72± 0.03	1.18 ± 0.06	0.27	0.44 ± 0.01
10% Pt/C	10	85 ± 4	1.96 ± 0.07	0.23 ± 0.01	0.20	0.61 ± 0.02

[a] exchange current density normalized by geometric surface area of the electrode.
[b] exchange current density normalized by Pt ECSA.
[c] exchange current density normalized by mass of Pt.
[d] transfer coefficient

References for the Electronic Supplementary Information

[S1] Y. Shen, A. C. Lua, J. Xi and X. Qiu, *ACS Appl. Mater. Interfaces,* 2016, **8**, 3464.

[S2] K. Elbert, J. Hu, Z. Ma, Y. Zhang, G. Chen, W. An, P. Liu, H. S. Isaacs, R. R. Adzic and J. X. Wang, *ACS Catal.,* 2015, **5**, 6764.

[S3] L. Wang, C. Lin, D. Huang, J. Chen, L. Jiang, M. Wang, L. Chi, L. Shi and J. Jin, *ACS Catal.,* 2015, **5**, 3801.

[S4] H. Yin, S. Zhao, K. Zhao, A. Muqsit, H. Tang, L. Chang, H. Zhao, Y. Gao and Z. Tang, *Nat. Commun.,* 2015, **6**, 6430.

[S5] R. Subbaraman, D. Tripkovic, D. Strmcnik, K.-C. Chang, M. Uchimura, A. P. Paulikas, V. Stamenkovic and N. M. Markovic, *Science,* 2011, **334**, 1256.

[S6] M. Smiljanic, Z. Rakocevic, A. Maksic and S. Strbac, *Electrochim. Acta,* 2014, **117**, 336.

[S7] E. G. Mahoney, W. Sheng, Y. Yan and J. G. Chen, *ChemElectroChem,* 2014, **1**, 2058.

[S8] S. M. Alia, B. S. Pivovar and Y. Yan, *J. Am. Chem. Soc.,* 2013, **135**, 13473.

[S9] R. Subbaraman, D. Tripkovic, K.-C. Chang, D. Strmcnik, A. P. Paulikas, P. Hirunsit, M. Chan, J. Greeley, V. Stamenkovic and N. M. Markovic, *Nat. Mater.,* 2012, **11**, 550.